

Observation of Broadband Self-Amplified Spontaneous Coherent Terahertz Synchrotron Radiation in a Storage Ring

J. M. Byrd,^{1,2} W. P. Leemans,¹ A. Loftsdottir,^{1,2} B. Marcellis,¹ Michael C. Martin,¹ W. R. McKinney,¹
F. Sannibale,¹ T. Scarvie,¹ and C. Steier¹

¹*Lawrence Berkeley National Laboratory, One Cyclotron Road, Berkeley, California 94720*

²*Department of Physics, University of California, Davis, Davis, California 95616*

(Received 9 August 2002; published 8 November 2002)

Bursts of coherent synchrotron radiation at far-infrared and millimeter wavelengths have been observed at several storage rings. A microbunching instability has been proposed as the source for the bursts. However, the microbunching mechanism has yet to be elucidated. We provide the first evidence that the bursts are due to a microbunching instability driven by the emission of synchrotron radiation in the bunch. Observations made at the Advanced Light Source are consistent with the values predicted by the proposed microbunching model. These results demonstrate a new instability regime for high energy synchrotron radiation sources and could impact the design of future sources.

DOI: 10.1103/PhysRevLett.89.224801

PACS numbers: 41.60.Ap, 29.20.-c, 41.75.Ht

Synchrotron radiation is generated by high energy electron beams accelerated by magnetic bending fields. Coherent synchrotron radiation (CSR) occurs when the emission of multiple electrons in a bunch is in phase, resulting in a quadratic dependence of the power emitted on the number of electrons participating. CSR is possible when either the entire electron bunch or any longitudinal structure of the bunch is comparable to the radiation wavelength [1,2]. CSR has been a subject of great interest for some time to both the synchrotron radiation and accelerator design communities. The quadratic dependence of radiated power on the beam current promises a significant new source in the terahertz region. However, the effect of the coherent emission on the electron beam could result in a self-amplified instability, resulting in large pulse-to-pulse variations, thereby limiting the potential application of the CSR as a useful source.

There have been several reports of quasiperiodic bursts of CSR in the microwave and far-infrared range [3–7]. The mechanism for these bursts is not yet well understood. Recently, a model to explain these effects has been proposed [8]. In this model, the interaction of the beam with its own synchrotron radiation creates microbunching within the electron bunch which then amplifies itself via coherent emission. It has been postulated that the subsequent growth and decay of the microbunching instability results in a series of bursts of CSR. Further simulation studies of this model suggest that periodic bursts are a signature of this instability [9]. This effect may have implications for the operations of present and future storage rings and may present an ultimate limit on the peak current density of a bunch that can be achieved.

In principle, CSR occurs at a radiation wavelength comparable to the bunch length. However, long wavelength synchrotron radiation is suppressed by a wave-

guide cutoff condition imposed by the vacuum chamber. For most modern electron rings, this cutoff occurs between a few millimeters to a few hundred microns. One of the difficulties in achieving steady CSR has been to reach bunch lengths shorter than these values [10].

In this Letter, we present the first experimental evidence indicating that the instability thresholds predicted by the microbunching model correspond to the observed thresholds for the CSR bursts. We have measured the CSR bursts at the Advanced Light Source (ALS), a 1.9 GeV electron storage ring. The instability threshold was measured at two wavelengths for different electron beam energies and bunch lengths. These data show good agreement with the model.

Far-infrared measurements were carried out at the ALS IR beam line 1.4 [11–13]. This beam line collects 10-mrad vertical by 40-mrad horizontal of bend-magnet synchrotron radiation. The source is reimaged by an off-axis ellipsoid with 3.5 m conjugate distances. The light is passed either through a chemical vapor deposition diamond window for Fourier transform infrared (FTIR) spectral measurements or a fused silica window for time-domain measurements with one of three far-IR detectors. FTIR spectra were acquired using a standard commercial far-infrared FTIR spectroscopy system (Bruker 66v/S) spectrometer using a 26-micron Mylar beam splitter and an Infrared Laboratories 4.2 K Si bolometer with a 100 cm⁻¹ cut-on filter. Time-domain measurements of the far-IR emissions were made using the same 4.2 K bolometer or a 1.6 K IR Labs Si bolometer with a 40 cm⁻¹ Fluorogold cut-on filter. To measure at even longer wavelengths, a 94 GHz microwave detector system was used consisting of two rf diodes: an Impatt diode operating at 94 GHz and a Gunn diode that can be frequency tuned and locked at a specific frequency difference with the Impatt diode. This diode signal is mixed

with the Impatt and incoming signal, providing a signal at the difference frequency of ~ 500 MHz. The output signals of all three detector systems were monitored with an oscilloscope.

Examples of the signal observed on the 4.2 K bolometer during bursting are shown in Figs. 1(a)–1(c). Above a threshold single bunch current, bursts of signal appear. The bolometer has a rise and fall time of 50 and 500 μ sec, respectively. Each of the individual bursts shows this characteristic time response. As the current increases, the burst signals increase in both amplitude and frequency. The polarization of the radiation was measured to be entirely in the plane of the electron beam orbit, consistent with the expected polarization level of greater than 99.5%. At the highest single bunch current, the bursts appear almost continuously, often large enough to saturate the bolometer. At 27–31 mA, the bursts develop a periodic envelope as shown in Fig. 1(b). The examples shown here are typical of the signals observed on all three detectors.

A measurement of the average spectral content of the bursts using the 4.2 K bolometer and Bruker 66v/S is shown in Fig. 2. All spectra are normalized to the thermal background signal (zero beam current) in order to mini-

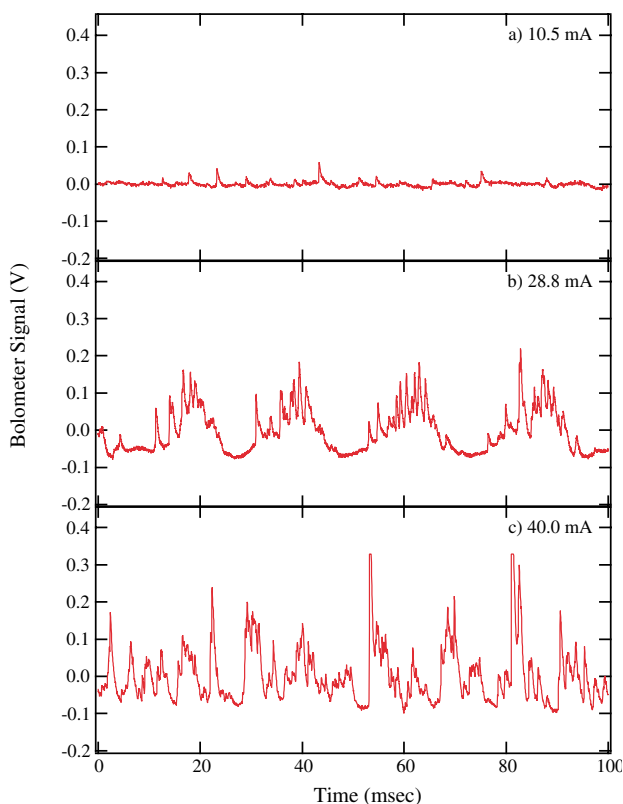


FIG. 1 (color online). Bolometer signal measured demonstrating bursting above threshold at three current values. Between 27 and 31 mA the bursts develop a periodic behavior. Above this current they appear more chaotic.

mize the response of the spectrometer, beam splitter, and detector. The signal shows up to a hundredfold increase at wave numbers below 30 cm^{-1} ($\lambda > 333 \mu\text{m}$). The inset shows the integrated signal in the spectrum from $15\text{--}40 \text{ cm}^{-1}$. A fit to a zero-offset quadratic is also shown, confirming that this signal is coherent.

The time-averaged signal on the 1.6 K bolometer as a function of current for both single bunch and multibunch filling of the ring is shown in Fig. 3. Because the multibunch beam current is distributed among 300 bunches, the bunch current is well below the threshold for any instabilities, and the radiation signal is expected to be incoherent and show a linear dependence on current. Below the bursting threshold, the single bunch signal shows a dependence on current greater than linear and magnitude significantly higher than the multibunch signal at the same current. We believe this is an indication of stable CSR. At the threshold for observing bursts, the data shows an exponential increase which eventually shows some saturation at higher bunch currents.

Heifets and Stupakov have developed a model which predicts a microbunching instability excited by coherent synchrotron radiation in electron rings [8]. The model starts from the observation that fluctuations in the longitudinal bunch distribution, with characteristic length much shorter than the bunch length, can radiate coherently. Under proper conditions, the CSR emission can increase the fluctuation, triggering a chain effect leading to microbunching and instability. The possible wavelengths for CSR bursting are limited by vacuum chamber shielding that sets an upper limit and by the bunch energy spread which, for shorter wavelengths, generates a longitudinal “remixing” that opposes the growth of the microbunching. From the theory a criterion that gives a current threshold for the instability and the CSR bursting can be

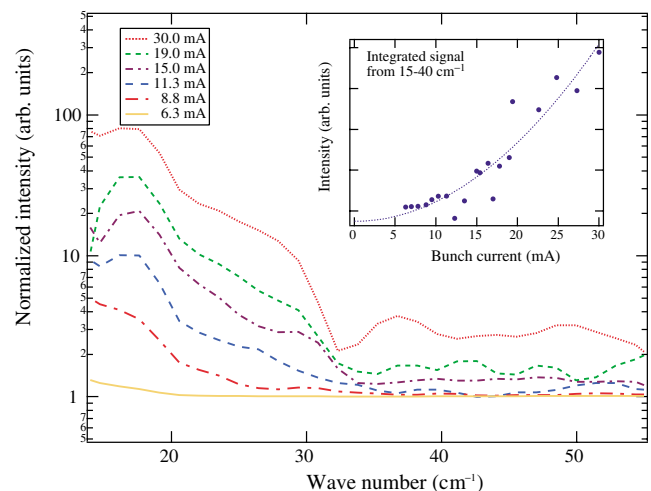


FIG. 2 (color online). Average frequency spectrum of bursts as a function of current. Inset: the integrated signal shows a quadratic dependence of the signal.

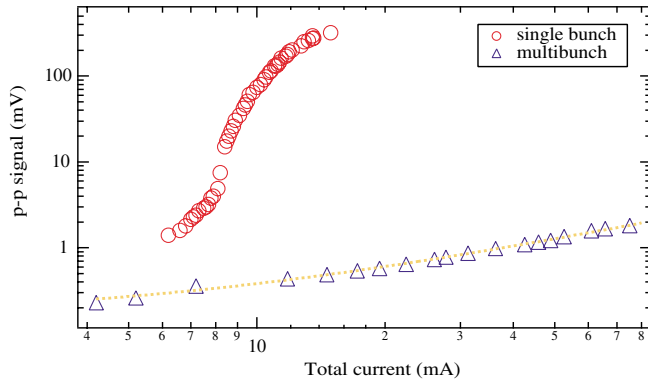


FIG. 3 (color online). 1.6 K bolometer signal as a function of total current for single and multibunch operation. The multibunch beam current is distributed into 300 bunches. The dashed line is a linear fit to the multibunch signal.

derived:

$$I_b > \frac{\pi^{1/6} e c}{\sqrt{2} r_0} \frac{\gamma}{\rho^{1/3}} \alpha \delta_0^2 \sigma \frac{1}{\lambda^{2/3}}, \quad (1)$$

where I_b is the average current per bunch, e is the electron charge, c is the speed of light, r_0 is the electron classical radius, γ is the beam energy in units of the rest mass, ρ (4.96 m) is the dipole bending radius, α ($1.37e - 3$) is the momentum compaction, δ_0 is the relative energy spread, σ is the rms bunch length, and λ is the wavelength of the perturbation. Equation (1) holds for a Gaussian distribution with $\sigma > \lambda/2\pi$ and for a wavelength λ less than the evanescent waveguide cutoff for the vacuum chamber.

The quantities δ and σ implicitly depend on γ , ρ , and on other machine parameters. If a nonmicrowave instability regime is assumed, then the expressions for the natural bunch length and energy spread can be used in Eq. (1) to obtain:

$$I_b > A \frac{1}{f_0 h^{1/2} V_{rf}^{1/2} [1 - (U_0/eV_{rf})^2]^{1/4}} \frac{\alpha^{3/2}}{\rho^{11/6} J_s^{3/2}} \frac{\gamma^{9/2}}{\lambda^{2/3}}, \quad (2)$$

where $A = (m_0 e c^6 C_q^3)^{1/2} / 2\pi^{1/3} r_0$, m_0 is the electron mass, h (328) is the harmonic number, f_0 (1.5233 MHz) is the revolution frequency, V_{rf} (1.3 MV) is the rf peak voltage, J_s (1.75) is the longitudinal partition number, and $C_q = 3.832 \times 10^{-13}$ m. The dependence of the radiation loss per turn, U_0 , on γ and bending radius can be ignored when $U_0/eV_{rf} \ll 1$.

In a recent upgrade of the ALS, superconducting bending magnets have replaced 3 of the 36 normal conducting ones. The new dipoles maintain the same bending angle but have different radius (1.46 m). In this case, the expressions for the bending radius in Eqs. (1) and (2) must be replaced by

$$\rho^{1/3} = (\rho_{sc}^{1/3} + 11\rho_n^{1/3})/12 \quad (3)$$

and

$$\rho^{11/6} = \frac{(\rho_{sc}^{1/3} + 11\rho_n^{1/3})}{12} \left(\frac{\rho_{sc} \rho_n (\rho_n + 11\rho_{sc})}{\rho_n^2 + 11\rho_{sc}^2} \right)^{3/2}, \quad (4)$$

where ρ_n and ρ_{sc} are the radii of the normal and superconducting magnets.

To compare the bursting instability with the model, we measured the bursting threshold as a function of electron beam energy. The results are shown in Fig. 4. The points with error bars indicate the experimental data, while the solid lines show the theoretical threshold calculated using Eq. (2) for the nominal ALS parameters. The previously mentioned 94 GHz detector and the 1.6 K Si bolometer were used for the two different wavelength measurement sets. For the 94 GHz detector, which has a narrow band response of 1 GHz, the center value of $\lambda = 3.2$ mm was used for calculating the theoretical curve in Fig. 4. For the bolometer, the lower limit (larger wavelength value) of its bandwidth, 0.5–2 mm, was used for the purpose. This assumption can be justified by the fact that the instability theory indicates that CSR bursting thresholds are smaller for larger wavelengths. Because of insufficient sensitivity, the 94 GHz detector was not able to detect any signal below threshold. This introduces an overestimate of the measured current threshold. The asymmetric error bars in Fig. 4 on the 94 GHz detector data account for this effect. On the contrary, the sensitivity of the 1.6 K bolometer allowed a clear measurement also in the absence of CSR bursting; see Fig. 4. For this case, we define the bursting threshold current value where the measured intensity deviates from linearity as shown in Fig. 3.

The agreement between theory and experimental data is remarkably good for the 94 GHz detector case, especially since no parameters were adjusted to reach

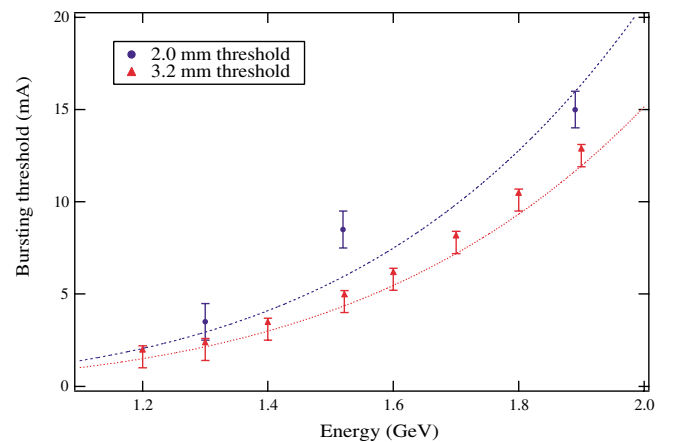


FIG. 4 (color online). Bursting threshold as a function of electron beam energy at 3.2 and 2 mm wavelengths. Data are shown as points. Calculated threshold using nominal ALS parameters at 3.2 and 2 mm wavelengths are shown as dashed lines.

agreement. The agreement is reasonably good for the bolometer. At higher bunch currents, we expect the bunch energy spread and length to increase from the nominal values due to effects from the vacuum chamber impedance such as potential well distortion and microwave instabilities. Therefore, the agreement at these currents, corresponding to shorter wavelengths, will be worse than at lower currents.

One of the primary difficulties in distinguishing a microbunching instability driven by CSR from that driven by a vacuum chamber impedance (i.e., bellows, etc.) is that the dependence of the threshold depends solely on the value of the impedance. We believe there are several features of our measurements which favor the CSR interpretation. First, the large bandwidth of the signals as shown in Fig. 2 supports a broadband source of impedance, consistent with the radiation impedance. Another mechanism that could mimic the burst signals is a microwave instability at a lower frequency which generates higher harmonics via nonlinear saturation of the instability. Second, we have searched for such an instability up to a frequency of 10 GHz and have found none which show a time structure comparable with the bursts as shown in Fig. 1. Finally, given the fundamental nature of the radiation impedance and the agreement of the data with the predicted thresholds, we believe this is a strong indication that the instability is driven by CSR.

We acknowledge the ALS operations staff for assistance with the measurements. This work was supported by the Director, Office of Science, of the U.S. Department of Energy under Contract No. DE-AC03-76SF00098.

- [1] J.S. Nodvick and D.S. Saxon, *Phys. Rev.* **96**, 180 (1954).
- [2] G. Williams *et al.*, *Phys. Rev. Lett.* **2**, 261 (1989).
- [3] U. Arp *et al.*, *Phys. Rev. ST Accel. Beams* **4**, 054401 (2001).
- [4] G. L. Carr, S. L. Kramer, J. B. Murphy, R. P. S. M. Lobo, and D. B. Tanner, *Nucl. Instrum. Methods Phys. Res., Sect. A* **463**, 387 (2001).
- [5] Å. Andersson, M. Johnson, and B. Nelander, *Opt. Eng.* **39**, 3099–3105 (2000).
- [6] M. Abo-Bakr, J. Feikes, K. Holldack, D. Ponwitz, and G. Wüstefeld, in *Proceedings of the 2000 European Particle Acceleration Conference, June 2000, Vienna* (Austrian Academy of Sciences Press, Vienna, 2000).
- [7] B. Podobedov, G. L. Carr, S. L. Kramer, and J. B. Murphy, in *Proceedings of the 2001 Particle Acceleration Conference, June 2001, Chicago* (IEEE, Piscataway, NJ, 2001).
- [8] S. Heifets and G. Stupakov, *Phys. Rev. ST Accel. Beams* **5**, 054402 (2002).
- [9] M. Venturini and R. Warnock, *Phys. Rev. Lett.* (to be published).
- [10] M. Abo-Bakr, J. Feikes, K. Holldack, G. Wüstefeld, and H.-W. Hübers, *Phys. Rev. Lett.* **88**, 254801 (2002).
- [11] W. R. McKinney *et al.*, in *Accelerator-Based Infrared Sources and Applications*, SPIE Proceedings Vol. 3153 (SPIE-International Society for Optical Engineering, San Diego, 1997), p. 59.
- [12] W. R. McKinney *et al.*, in *Accelerator-Based Sources of Infrared and Spectroscopic Applications*, edited by G. L. Carr and P. Dumas, SPIE Proceedings Vol. 3775 (SPIE-International Society for Optical Engineering, Denver, CO, 1999), p. 37.
- [13] M. C. Martin and W. R. McKinney, *Ferroelectrics* **249**, 1 (2001).